Quantitative Airway Analysis in Longitudinal Studies Using Groupwise Registration and 4D Optimal Surfaces

Jens Petersen[1], Marc Modat[2], Manuel Jorge Cardoso[2], Asger Dirksen[3], Sebastien Ourselin[2], and Marleen de Bruijne[1,4]

[1] Image Group, Department of Computer Science, University of Copenhagen, Denmark
[2] Centre for Medical Image Computing, Department of Medical Physics and Bioengineering, University College London, United Kingdom
[3] Department of Respiratory Medicine, Gentofte Hospital, Denmark
[4] Biomedical Imaging Group Rotterdam, Departments of Radiology & Medical Informatics, Erasmus MC, Rotterdam, The Netherlands

Abstract. Quantifying local changes to the airway wall surfaces from computed tomography images is important in the study of diseases such as chronic obstructive pulmonary disease. Current approaches segment the airways in the individual time point images and subsequently aggregate per airway generation or perform branch matching to assess regional changes. In contrast, we propose an integrated approach analysing the time points simultaneously using a subject-specific groupwise space and 4D optimal surface segmentation. The method combines information from all time points and measurements are matched locally at any position on the resulting surfaces.

Visual inspection of the scans of 10 subjects showed increased tree length compared to the state of the art with little change in the amount of false positives. A large scale analysis of the airways of 374 subjects including a total of 1870 images showed significant correlation with lung function and high reproducibility of the measurements.

Keywords: CT, airway, lung, longitudinal, segmentation, registration.

1 Introduction

Assessing the dimensions and attenuation values of airway walls from Computed Tomography (CT) images is important in the investigation of airway remodelling diseases such as Chronic Obstructive Pulmonary Disease (COPD) [4]. Manual measurements are very time consuming and subject to intra- and inter-observer variability. Automatic methods are needed to estimate the dimensions of large parts of the airway tree. Obtaining reproducible measurements is difficult because of a strong dependence on position in what is a complicated biologically and dynamically varied tree-like structure. Previous approaches have solved the

K. Mori et al. (Eds.): MICCAI 2013, Part II, LNCS 8150, pp. 287–294, 2013.

problem in two steps: first a step, to segment the airways and conduct the measurements, and second a step to identify anatomical branches or match individual airway segments in multiple scans of the same subject [12,10,3]. The task of anatomically identifying airway branches poses significant problems even to medical experts [3]. Most automatic methods therefore do not go beyond the segmental level, resulting in 32 labelled branches [3,12]. State of the art segmentation methods can extract many more branches reliably [7], and intra-subject branch matching can thus increase the information available in longitudinal studies. It has been done using image registration [10], or association graphs [12].

A limitation of such two-step approaches is that longitudinal information is not used to the fullest. For instance branches need to be segmented in every scan in order to be matched even though a branch that is detected in one scan is most likely present in all. The proposed method improves on this by segmenting multiple scans of the same subject simultaneously. It is thus able to combine information from all time points and enables matched measurements, not just at the branch level, but locally at any point on the resulting surfaces.

2 Methods

An initial airway lumen probability map (section 2.2) was constructed by transferring initial segmentations of each time point to a per-subject common space constructed through deformable image registration (section 2.1). A four dimensional optimal surface graph was built from the initial probability map and used to find the inner and outer airway wall surfaces as the global optimum of a cost function combining image terms with surface smoothness, surface separation, and longitudinal penalties and constraints (section 2.3).

2.1 Groupwise Registration of Images

Prior to registration, intensity inhomogeneity due to for instance gravity gradients and ventilation differences was removed within the lungs using the NiftySeg software (`http://sourceforge.net/projects/niftyseg`) [2]. The approach is using a two-class expectation-maximization based probabilistic framework, which incorporates both a Markov Random field spatial smoothness term and an intra-class intensity inhomogeneity correction step.

All registrations have been performed with a stationary velocity field parametrisation and using normalised mutual information as a measure of similarity with the NiftyReg software (`http://sourceforge.net/projects/niftyreg`) [8]. For each subject, all time points were aligned to the Frechet mean on the space of diffeomorphisms, thus providing a common space for analysis and a one-to-one mapping between time points.

2.2 Initial Segmentation

An initial airway lumen segmentation was obtained in each individual image using the Locally Optimal Path (LOP) approach of [6]. Segmentations from every scan of the same subject were then warped to the subject-specific groupwise

space and averaged, giving a lumen probability map. By thresholding this using some value T, it is possible to move freely between the intersection and union of the segmentations, weighting the amount of included branches against the amount of false positives. Disconnected components were connected along centrelines extracted from the union segmentation using the method described in [7]. The voxel based initial segmentation was then converted to triangle mesh with vertices $\mathcal{V}$ and edges $\mathcal{E}$, using the marching cubes algorithm.

2.3 Graph Construction

This section describes how a graph $G = (V, E)$ can be constructed, such that the minimum cut of G defines the set of surfaces $M = \mathcal{I} \cup \mathcal{O}$ where $\mathcal{I} = \{\mathcal{I}_0, \mathcal{I}_1, \ldots, \mathcal{I}_N\}$ and $\mathcal{O} = \{\mathcal{O}_0, \mathcal{O}_1, \ldots, \mathcal{O}_N\}$ are the inner and outer surfaces of the N scans of the subject. The graph is similar to that of [11], the differences being the addition of the longitudinal connections and hard constraints.

The vertices of the graph are defined by a set of columns V_i^m one for each vertex $i \in \mathcal{V}$ of the initial mesh and sought surface $m \in M$, and a source s and a sink vertex t. As in [11] we will let the columns be defined from sampled flow lines traced inward and outward from $i \in \mathcal{V}$. Because they are non-intersecting, the found solutions are guaranteed to not self-intersect. Tracing is done within a scalar field arising from the convolution of the binarised initial segmentation with a Gaussian kernel of scale σ. Sampling is done at regular arc length intervals relative to i until tracing is stopped due to flattening of the gradient, giving I_i and O_i inner and outer column points. So, $V_i^m = \{i_k^m \mid k \in K_i\}$, where $K_i = \{-I_i, 1 - I_i, \ldots, 0, \ldots, O_i\}$ and $V = \bigcup_{i \in \mathcal{V}, m \in M} V_i^m \cup \{s, t\}$. In this way, the column defines the set of all possible solutions for i in the surface m.

Let $(v \xrightarrow{c} u)$ denote a directed edge from vertex v to vertex u with capacity c and $w_i^m(k) \geq 0$ be a cost function, giving the cost of vertex k in a column V_i^m being part of the surface m. This data term can be implemented by the edges:

$$E_d = \Big\{ \big\{ (i_k^m \overset{w_i^m(k)}{\rightarrow} i_{k+1}^m) \mid k, k+1 \in K_i \big\} \cup \big\{ (i_{O_i}^m \overset{w_i^m(O_i)}{\rightarrow} t), (s \overset{\infty}{\rightarrow} i_{I_i}^m) \big\} \mid i \in \mathcal{V}, m \in M \Big\} . \tag{1}$$

To prevent degenerate cases where a column is cut multiple times and to preserve topology, the following infinite cost edges are added:

$$E_\infty = \Big\{ (i_k^m \overset{\infty}{\rightarrow} i_{k-1}^m) \mid \ i \in \mathcal{V}, m \in M, k-1, k \in K_i \Big\} . \tag{2}$$

An example of these edges is given in figure 1(a).

Let $f_{i,j,m,n}(|k - l|)$ be a convex non-decreasing function giving the pairwise cost of both $i_k^m \in V_i$ and $j_l^n \in V_j$ being part of the surfaces $m, n \in M$ respectively. This can be used to implement surface smoothness and longitudinal penalties, see (equation 7). Additionally let the set $I(i_k^m, j, n) = \{\zeta, \zeta + 1, \ldots, \eta\} \subseteq \{-I_j, 1 - I_j, \ldots, O_j\}$ put pairwise constraints on the solution, such that if i_k^m and j_l^n

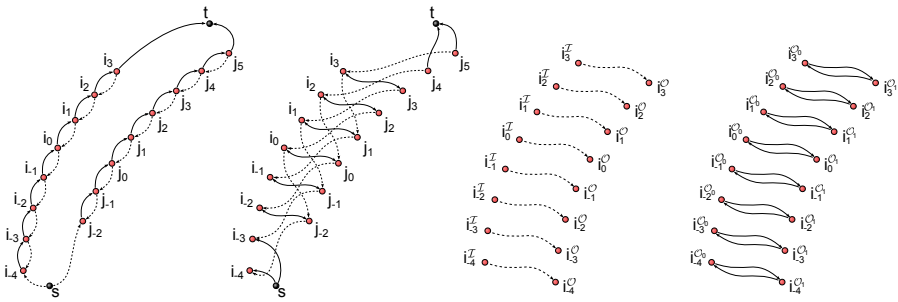

(a) Data and topology (b) Smoothness (c) Separation (d) Longitudinal

Fig. 1. Example columns with $I_i = 4$, $I_j = 2$, $O_i = 3$ and $O_j = 5$ inner and outer vertices illustrating the graph as implemented. The dotted edges have infinite capacity and implement hard topology, smoothness and separation constraints. The solid edge capacities are given by data term, smoothness, separation and longitudinal penalties.

are both part of it, then $l \in I(i_k^m, j, n)$. Such penalties and constraints can be implemented by:

$$\begin{aligned} E_i = \Big\{ & \big\{ (i_k^m \overset{\triangle(i_k^m, j_l^n)}{\rightarrow} j_l^n) \mid k \in K_i, l \in K_j \big\} \cup \\ & \big\{ (s \overset{\triangle(i_k^m, j_l^n)}{\rightarrow} j_l^n) \mid l \in K_j, k \in K_j, k < -I_i \big\} \cup \\ & \big\{ (i_k^m \overset{\triangle(i_k^m, j_l^n)}{\rightarrow} t) \mid k \in K_i, l \in K_i, l > O_j \big\} \\ & \mid i, j \in \mathcal{V}, m, n \in M \Big\} , \end{aligned} \tag{3}$$

and $\triangle$ gives the capacity of the edges as follows:

$$\triangle(i_k^m, j_l^n) = \begin{cases} \infty & \text{if } l = \min I(i_k^m, j, n) \\ 0 & \text{if } l \notin I(i_k^m, j, n) \\ \hat{\triangle}(k-l) & \text{otherwise} \end{cases} \tag{4}$$

where

$$\hat{\triangle}(x) = \begin{cases} 0 & \text{if } x < 0 \\ f_{i,j,m,n}(1) - f_{i,j,m,n}(0) & \text{if } x = 0 \\ f_{i,j,m,n}(x+1) - 2f_{i,j,m,n}(x) + f_{i,j,m,n}(x-1) & \text{if } x > 0. \end{cases} \tag{5}$$

Similar to the approach of [5], hard constraints was used to force the outer surfaces to be outside their corresponding inner surfaces and solutions to not vary more than γ and δ indices in neighbouring columns in the inner and outer surfaces as follows:

$$I(i_{k,m}, j, n) = \begin{cases} \{k, k+1, \ldots, O_j\} & \text{if } m \in \mathcal{I}_s \text{ and } n \in \mathcal{O}_s, \\ & s \in \{0, 1, \ldots, N\} \\ \{k-\gamma, k-\gamma+1, \ldots, k+\gamma\} & \text{if } m = n, \text{ and } n, m \in \mathcal{I} \\ \{k-\delta, k-\delta+1, \ldots, k+\delta\} & \text{if } m = n, \text{ and } n, m \in \mathcal{O} \\ K_j & \text{otherwise.} \end{cases} \tag{6}$$

The following pairwise cost were implemented:

$$f_{i,j,m,n}(x) = \begin{cases} p_m x \text{ if } m = n \text{ and } (i,j) \in \mathcal{E} \\ qx \quad \text{if } i = j \text{ and } m \in \mathcal{I}_s, n \in \mathcal{I}_{s+1} \text{ or } m \in \mathcal{O}_s, n \in \mathcal{O}_{s+1} \\ 0 \quad \text{otherwise.} \end{cases} \tag{7}$$

p_m is the smoothness penalty, defining the cost of each index the solution varies between neighbouring columns in the same surface m. q is the longitudinal penalty, defining the cost inherent in the solution for each index corresponding surfaces are separated in each column within the groupwise space. An illustration of these edges is given in figure 1(b) and 1(c). The total edge set E is given by: $E = E_d \cup E_\infty \cup E_i$.

The cost functions $w_k^m(k)$ were set to the first order derivative of the image intensity in the outward and inward direction of the flow line for the inner and outer surfaces respectively.

We used the algorithm described in [1] to find the minimum cut.

3 Experiments and Results

3.1 Data

CT images and lung function measurements from the Danish lung cancer screening trial [9] were used. Images were obtained using a Multi Detector CT scanner (Philips Mx 8000) with a low dose (120 kV and 40 mAs), reconstructed using a hard kernel (D) with a resolution of approximately 0.78 mm $\times$ 0.78 mm $\times$ 1 mm. The subjects (at inclusion) were men and women, former and current smokers with at least 20 pack years smoked, between 50 and 70 years of age and thus at high risk of having COPD.

We used images of 10 subjects for estimation of the parameters and evaluation of the process of merging the initial segmentations. An independent set of 374 subjects was used to evaluate the ability of the method to detect longitudinal changes in airway dimensions. From each subject 5 yearly scans were included out of which 1739 had matching lung function measurements.

3.2 Parameters and Merging of Initial Segmentations

The centrelines of the 10 subjects were moved from the groupwise space to the space of the last time point scan, in which they were manually checked using in-house developed software. The software allows movement along the centrelines while displaying a cross-sectional view of the airway.

Figure 2(a) and 3(a) show results of varying T - significantly more branches can be found by fusing information from multiple scans ($p < 0.05$ for $T < 0.4$), while the percentage of false positives does not seem to increase much. We chose a value of $T > 0.2$ corresponding to branches present in at least two scans.

Parameters were estimated by aiming to penalize and constrain solutions as little as possible while still preventing noisy segmentations and the inclusion of

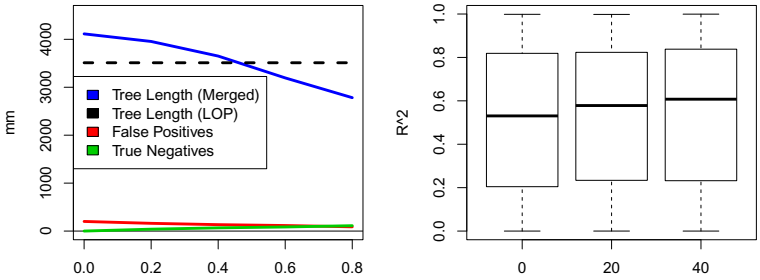

(a) Threshold (b) Longitudinal penalty

Fig. 2. Left: Average tree length for different values of the threshold T (blue), average tree length of the LOP segmentation as a comparison (black dashed), false positives (red) and true negatives (green) with respect to the union of the segmented branches. Right: the R^2 fit of the relative change in lung volume predicted from relative change in lumen diameter in each subject with increasing amount of longitudinal penalty.

abutting vessels. The mesh edges were roughly 0.4 mm apart and the flow lines were sampled at 0.4 mm spacings. p_m was set to 15 for all $m \in M$, γ and, δ to 2 and σ to 0.7 based on visual inspection of results. Figure 3(b) shows a segmentation result illustrated at two time points.

3.3 Longitudinal Segmentation

Experiments were conducted on the images of the 374 subjects with values $q \in \{0, 20, 40\}$ of the longitudinal penalty to assess its impact on the method's ability to detect changes in airway dimensions over time. Note that a value of 0 is similar to performing multiple independent (3D) searches, but with the added bonus that the solution meshes will have corresponding vertices. Measures of Wall Area percentage (WA%) and Lumen Diameter (LD) were computed from the average distance of the mesh vertices to the branch centreline, which was extracted from the average segmentation in the groupwise space and transformed to each individual time point. This enables accurate assessment of subtle localized changes in airway morphology, but to evaluate the performance of our segmentation to automatically derive known airway imaging biomarkers, we averaged the measures extracted in the airways of generation 3 to 6.

WA% was found to correlate significantly with lung function at each time point (Average Spearman's ρ: -0.29 ± 0.01, $p < 0.0001$). Different values of q did not change the results significantly. Reproducibility, quantified by correlating results at time point one with those of time point two with $q = 0$, was high: (Spearman's ρ: 0.95, 0.94, 0.89 and 0.85 in generation 3, 4, 5 and 6 respectively $p < 0.0001$). As expected, increasing q made the reproducibilities go towards 1.

Annual changes of WA% were found to be 0.31 ± 4.9 % significantly different from 0 (Mann-Whitney U test $p < 0.001$) with $q = 0$. Significance disappeared with $q \in \{20, 40\}$ perhaps evidence that these values are over-penalizing the solutions. No correlation was found between annual changes in WA% and annual

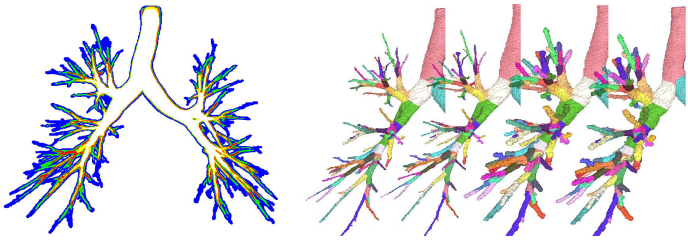

(a) (b)

Fig. 3. Left: initial segmentation example, at $T > 0$ (blue), $T > 1/5$ (green), $T > 2/5$ (red), $T > 3/5$ (yellow), and $T > 4/5$ (white). Right: inner followed by outer surface segmentations at two corresponding time points. Colors show matching branches.

changes in lung function. This is not surprising giving the relative slow developing nature of COPD and the known poor reproducibility of lung function measurements. It is similar to what was previously reported [10].

LD is dependent on the inspiration level and investigating the method's ability to detect this dependency can therefore be used as a surrogate for a much slower pathological change. The relative change in lung volume was thus predicted from the relative change in LD in each subject. The R^2 of all the models showed significantly better fit when using higher values of q ($p < 0.0001$ using Wilcoxon signed rank test), see figure 2(b), indicating that the chosen longitudinal penalties can improve the ability to detect changes in the inner surface.

4 Discussion and Conclusion

We have presented a method for the analysis of airways designed to fully exploit longitudinal imaging data. The method, in contrast to state of the art, can use information from all time points and because it outputs surface meshes with one-to-one correspondences between vertices, enables measurements to be compared locally without the need for a separate branch matching step. A visual evaluation of the scans of 10 subjects showed the method found significantly more complete airway trees with minimal changes to the false positive percentage. Results on 1870 scans show significant correlation with lung function and highly reproducible results. Future work will have to better investigate choices for the longitudinal penalty. For instance it is possible, as indicated by the experiments, that different values are needed for the inner and outer surfaces, due to the different contrast values between lumen and wall and between wall and lung parenchyma. It should also be noted that averaging measurements over large parts of the airway tree, as done in this work, is ignoring information provided by the matched measurements, however to limit the scope of the paper we left it to future work to develop statistical models incorporating this information. Such models should, we expect, have more power to detect changes.

Acknowledgements. This work was partly funded by EPSRC (EP/H046410/1), the National Institute for Health Research University College London Hospitals Biomedical Research Centre (Award 168), the Netherlands Organisation for Scientific Research (NWO), and AstraZeneca Sweden.

References

1. Boykov, Y., Kolmogorov, V.: An experimental comparison of min-cut/max- flow algorithms for energy minimization in vision. IEEE TPAMI 26(9), 1124–1137 (2004)
2. Cardoso, M.J., Clarkson, M.J., Ridgway, G.R., Modat, M., Fox, N.C., Ourselin, S.: Load: A locally adaptive cortical segmentation algorithm. NeuroImage 56(3), 1386–1397 (2011)
3. Feragen, A., Petersen, J., Owen, M., Lo, P., Thomsen, L.H., Wille, M.M.W., Dirksen, A., de Bruijne, M.: A hierarchical scheme for geodesic anatomical labeling of airway trees. In: Ayache, N., Delingette, H., Golland, P., Mori, K. (eds.) MICCAI 2012, Part III. LNCS, vol. 7512, pp. 147–155. Springer, Heidelberg (2012)
4. Hackx, M., Bankier, A.A., Gevenois, P.A.: Chronic obstructive pulmonary disease CT quantification of airways disease. Radiology 265(1), 34–48 (2012)
5. Liu, X., Chen, D.Z., Tawhai, M., Wu, X., Hoffman, E., Sonka, M.: Optimal graph search based segmentation of airway tree double surfaces across bifurcations. IEEE TMI (2012)
6. Lo, P., Sporring, J., Pedersen, J.J.H., de Bruijne, M.: Airway tree extraction with locally optimal paths. In: Yang, G.-Z., Hawkes, D., Rueckert, D., Noble, A., Taylor, C. (eds.) MICCAI 2009, Part II. LNCS, vol. 5762, pp. 51–58. Springer, Heidelberg (2009)
7. Lo, P., van Ginneken, B., Reinhardt, J.M., Yavarna, T., de Jong, P.A., Irving, B., Fetita, C., Ortner, M., Pinho, R., Sijbers, J., Feuerstein, M., Fabijanska, A., Bauer, C., Beichel, R., Mendoza, C.S., Wiemker, R., Lee, J., Reeves, A.P., Born, S., Weinheimer, O., van Rikxoort, E.M., Tschirren, J., Mori, K., Odry, B., Naidich, D.P., Hartmann, I., Hoffman, E.A., Prokop, M., Pedersen, J.H., de Bruijne, M.: Extraction of Airways from CT (EXACT 2009). IEEE TMI 31, 2093–2107 (2012)
8. Modat, M., Ridgway, G.R., Taylor, Z.A., Lehmann, M., Barnes, J., Hawkes, D.J., Fox, N.C., Ourselin, S.: Fast free-form deformation using graphics processing units. Comput. Methods Programs Biomed. 98(3), 278–284 (2010)
9. Pedersen, J.H., Ashraf, H., Dirksen, A., Bach, K., Hansen, H., Toennesen, P., Thorsen, H., Brodersen, J., Skov, B.G., Døssing, M., Mortensen, J., Richter, K., Clementsen, P., Seersholm, N.: The danish randomized lung cancer CT screening trial–overall design and results of the prevalence round. J. Thorac. Oncol. 4(5), 608–614 (2009)
10. Petersen, J., Gorbunova, V., Nielsen, M., Dirksen, A., Lo, P., de Bruijne, M.: Longitudinal analysis of airways using registration. In: Fourth International Workshop on Pulmonary Image Analysis (2011)
11. Petersen, J., Nielsen, M., Lo, P., Saghir, Z., Dirksen, A., de Bruijne, M.: Optimal graph based segmentation using flow lines with application to airway wall segmentation. In: IPMI, pp. 49–60 (2011)
12. Tschirren, J., McLennan, G., Palágyi, K., Hoffman, E.A., Sonka, M.: Matching and anatomical labeling of human airway tree. IEEE TMI 24(12), 1540–1547 (2005)